Kinetics of surface alloy formation: Cu(100)-$c(2\times2)$Pd

T. D. Pope, K. Griffiths, V. P. Zhdanov,* and P. R. Norton
Interface Science Western, The University of Western Ontario, London, Ontario, Canada N6A 5B7
(Received 16 December 1993)

The kinetics of formation of the Cu(100)-$c(2\times2)$Pd surface alloy is studied by adsorption of $\frac{1}{2}$ ML of Pd on Cu(100) at 100 K followed by rapid heating up to selected anneal temperatures between 248 and 276 K. The domain-growth process is monitored via low-energy electron diffraction (LEED), Auger-electron spectroscopy, work-function measurements, and hydrogen thermal desorption. The initial stage of alloy formation, during which a considerable fraction of adsorbed Pd atoms replaces Cu atoms located in the first substrate layer, is found to be rapid and short. The subsequent late stages are slow. In the latter case, beam-profile measurements are consistent with self-similar domain growth. The corresponding analysis of the LEED peak intensity indicates that the growth law for the average domain radius has a power-law form with an exponent of $\frac{1}{8}$. The scaling arguments presented show that such a low value of the growth exponent can really occur if the Pd-Cu ordering of the Allen-Cahn type is limited by dissolution of Pd islands occurring via the Lifshits-Slyozov scenario. The activation energy for diffusion in the domain-growth regime is estimated to be ≈ 0.4 eV.

I. INTRODUCTION

Experimental[1,2] and theoretical[3,4] studies indicate that surface and interfacial alloying occurs in many metal-on-metal systems. Typically, the adsorbate forms an overlayer at low temperature and alloys with the substrate at higher temperatures. By rapid heating from the overlayer regime into the alloy regime, the kinetics of surface alloy formation may be studied. Physically, such kinetics can be described in terms of the theory of domain growth.

The early stages of the domain or island growth are known to be nonuniversal. However, shortly after a quench into an unstable state, the system usually develops local ordered domains. The kinetics of the domain growth then become dependent only on general parameters such as the number of equivalent ground states and the relevant conservation laws. By analogy with critical phenomena, the growth law for the average domain radius $R(t)$ in the late stage of phase transitions is usually assumed to have a power-law form

$$R(t)=At^{x}\ , \tag{1}$$

where x is the "universal" exponent. Equation (1) is based on the classical analytical results derived by Lifshits and Slyozov[5] for first-order phase transitions ($x=\frac{1}{3}$), and by Allen and Cahn[6] for continuous transitions with a doubly degenerate ground state ($x=\frac{1}{2}$). Numerous Monte Carlo simulations confirm these results and indicate that the growth exponent may in principle be lower than $\frac{1}{2}$ for systems with high-order ground-state degeneracy.[7,8]

Experimentally, the kinetics of the domain growth can be monitored by LEED, considering that the observed superlattice LEED peak height is proportional to $R^2(t)$,

$$I_0(t)\sim R^2(t)\ , \tag{2}$$

or, using Eq. (1),

$$I_0(t)\sim A^2t^{2x}\ . \tag{3}$$

The subscript 0 in $I_0(t)$ indicates that the intensity is measured in the center of the LEED beam, i.e., for a parallel momentum transfer of 0 from the Bragg maximum. Equation (2) was derived by employing formally the scaling hypothesis for the structure factor.[7] Physically, Eq. (2) is a consequence of fluctuations of the numbers of domains with different values of the order parameter in the area corresponding to coherent scattering.[8,9] Equation (2) has also been obtained by assuming that the LEED intensity is simply proportional to the total number of domains.[10] The latter approach, however, does not take into account the interference of electron scattering on domains with different values of the order parameter and ignores the fluctuation background of Eq. (2). Accordingly, it is not applicable for order-disorder phase transitions.

The measured growth exponents for phase transitions in adsorbed overlayers are as follows: W(110)-$p(2\times1)$O, $x=0.25-0.28$ (Refs. 10 and 11), W(110)-$[p(2\times1)+p(2\times2)]$O, $x=0.20-0.31$ (Refs. 10–12), W(112)-$p(2\times1)$O, $x=\frac{1}{2}$ (Ref. 13), Mo(110)-$p(2\times2)$S, $x=0.36$ (Ref. 14).

In the present paper, we describe the kinetics of formation of the Cu(100)-$c(2\times2)$Pd surface alloy. It is the first study of domain growth during surface alloy formation. The problem under consideration is of greater complexity than those explored for common adsorbate/substrate systems (e.g., oxygen on tungsten), because the Pd/Cu alloy formation is expected to occur via interlayer atomic exchange. In addition, the growth of the $c(2\times2)$Cu-Pd domains is accompanied, as discussed below, by two-dimensional evaporation of Pd atoms from Pd islands. In fact, there is a nontrivial interplay between these two kinetic channels.

0163-1829/94/50(24)/18553(11)/$06.00

The Cu(100)-$c(2\times2)$Pd surface alloy is known[2,4,15] to be formed when one-half monolayer (ML) of Pd is deposited on Cu(100) at 300 K. In our experiments, Pd was adsorbed at 100 K. In this case, Pd forms a poorly ordered overlayer with no $c(2\times2)$ superlattice intensity. Annealing the system at temperatures above 170 K again yields the $c(2\times2)$ structure. As discussed below, the appearance of $c(2\times2)$ superlattice beams correlates with the exchange of Pd atoms into the first substrate layer. The $c(2\times2)$ superlattice intensity thus originates only from alloy regions having the $c(2\times2)$ structure. We have studied the evolution of this structure at 248, 261, 268, and 276 K by measuring the time dependence of the intensity in the half-order LEED beams corresponding to the $c(2\times2)$ superlattice. Changes in the surface structure were also probed by AES, work-function measurements, and hydrogen chemisorption.

The presentation below is organized as follows. Experimental details are given in Sec. II. The LEED, AES, work-function and thermal-desorption data are exhibited in Sec. III. The interpretation of the results obtained (Sec. IV) includes a discussion of possible scenarios of domain growth and a scaling analysis of the most probable scheme. The observed kinetics are also compared with those of McRae and Malic[16] for the surface ordering of a bulk $Cu_3Au(110)$ alloy.

II. EXPERIMENT

The experiments were performed in a stainless-steel UHV chamber with a base pressure below 1×10^{-10} Torr. The chamber is equipped with a LEED optic, a cylindrical mirror analyzer with coaxial electron gun, a quadrupole mass spectrometer, a Kelvin work-function probe, a Pd evaporator, and provisions for gas exposure.

The crystal was cut from a boule and aligned by x-ray diffraction to within 0.5° of the (100) plane. It was polished with increasingly fine grades of diamond paste and finally with a 0.06-μm alumina slurry. The Cu(100) sample was mounted to the manipulator with 0.010-in. Ta wires fed through spark-machined holes in the crystal. The Ta wires were resistively heated to control the sample temperature. The crystal was initially sputtered and annealed at 1150 K until a sharp (1×1) LEED pattern was seen and no impurities were detectable by AES. After the initial sputtering treatment the crystal was routinely cleaned by two cycles of Ar ion sputtering (2 keV, 1 $\mu A/cm^2$, 20 min) followed by annealing for 20 min at 700 K.

Pd evaporation was done by electron bombardment of a Pd wire wrapped around a Ta support. Excellent reproducibility of the evaporation rate was achieved by using an evaporator power supply that regulated the emission current. The pressure in the chamber rose to $(5-8)\times10^{-10}$ Torr during evaporation, most of the impurity gas being hydrogen. The evaporation rate, determined by employing a previous Rutherford backscattering (RBS) calibration,[17] was 0.10 ± 0.01 ML/min.

Sample temperature was measured using a K-type thermocouple inserted into a hole in the side of the crystal. The temperature was controlled by a home-built temperature controller with feedback from the thermocouple. The heating rate, approximately 10 K/s, was limited to prevent temperature overshoot.

The LEED experiments were recorded on a video cassette recorder (VCR) using a silicon-intensified (SIT) camera focused on the LEED screen. The VCR was interfaced to a computer via an image-processing board. The 3D integrated spot intensities and 2D spot profiles were extracted employing software of our own design. A global background subtraction was performed using an image of the LEED screen at a beam energy of 0 eV. A local background subtraction routine discriminating the average pixel value in a narrow swath around the analysis window was also used. The beam intensities were normalized between experiments by employing the 3D integrated intensity of the (1,0) beam. The relative peak heights were calculated by dividing the 3D integrated intensity by the square of the full width at half maximum (FWHM). Separate measurements of the peak heights from the 2D profiles for some experiments confirmed the accuracy of this procedure.

The AES measurements were made at normal incidence with a primary beam energy of 2 keV. For the AES and work-function measurements, the spectrometer and Kelvin probe controller, as well as the temperature controller, were linked with a computer. The change in the work function or the differentiated Auger spectra could then be acquired at the same time as the sample temperature, about once per second. The effect of the heater current on the AES and work-function measurements was carefully nulled by employing data from blank experiments.

The thermal-desorption spectra were collected using a differentially pumped computer controlled VG SX300 quadrupole mass spectrometer. The computer could simultaneously acquire the sample temperature, change in work function, total pressure, and desorption signal for several masses. The spectrometer was fitted with a nozzle so that only the crystal face had a line of sight to the analyzer. Desorption spectra were typically recorded at a heating rate of 2 K/s.

The kinetic experiments proceeded as follows: 0.5 ± 0.05 ML of Pd were deposited on the Cu(100) surface at 100 K. The temperature was then ramped at 10 K/s to the desired value and thereafter held constant.

The cleanliness of the sample surface was checked by AES following the experiments. Any contaminants were below the detection limit of the spectrometer. This is reasonable given that the anneal temperatures are within the desorption range for CO and above the desorption range for water. Thermal-desorption measurements, however, reveal that during Pd deposition some hydrogen (≈0.20 ML) and CO (≈0.03 ML) are adsorbed. These contaminants are almost completely desorbed during the subsequent heating ramp.

III. RESULTS OF MEASUREMENTS

A. LEED

The time dependence of the integrated intensity of the half-order LEED beams measured at 276, 268, and 248 K

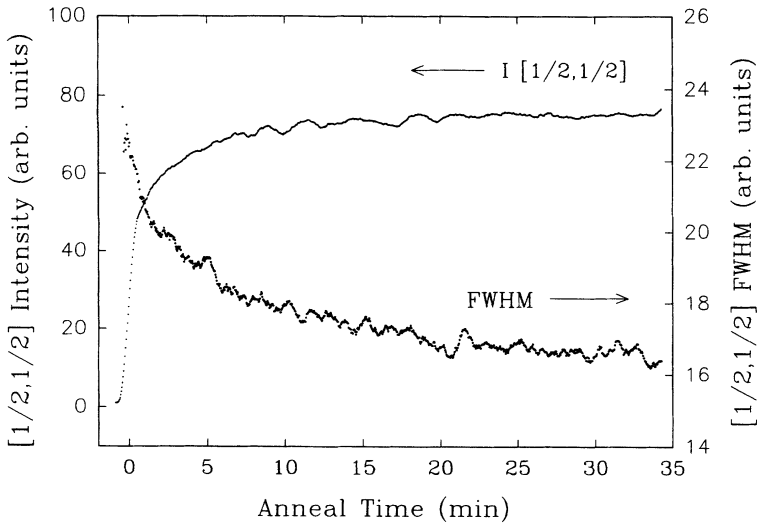

FIG. 1. Integrated intensity and full width at half maximum of the half-order beams as functions of anneal time at 276 K for 0.5 ML Pd on Cu(100).

are shown in Figs. 1 and 2. Figure 1 also exhibits the time dependence of the FWHM. In the temperature ramp region ($t<0$), the intensity rises rapidly with temperature. Once the anneal temperature is reached, the intensity continues to increase in a nonlinear manner. The initial stage of the domain growth is seen to be characterized by a very fast increase in the integrated intensity (due to rapid formation of small domains). The apparent activation energy for the initial slope of the integrated intensity, obtained from data like those shown in the inset of Fig. 2, is 0.34 ± 0.02 eV. With increasing time, the domain growth becomes much slower. The FWHM rapidly decreases early in the anneal and continues to decrease even when the integrated intensity has nearly saturated. For a given anneal time, higher anneal temperatures result in greater ultimate integrated intensity and smaller ultimate FWHM.

A series of LEED spot profiles taken at various times ($t>50$ s) during a 276-K anneal are shown in Fig. 3. The peak heights are normalized and the parallel momentum transfer is scaled by dividing by the FWHM. The true profiles are very broad relative to the instrument response function, so deconvolution of the instrument response function was not done. The profiles overlap one another, consistent with scaling behavior (self-similar growth). Profiles collected earlier in the anneal ($t<50$ s) appeared narrower along the abscissa suggesting a narrower distribution of domain sizes. Scaling behavior is not expected in this early regime.

For the late stages, when the domain growth is self-similar, the natural logarithm of the *peak height* as a function of the natural logarithm of the anneal time is found to form parallel straight-line segments (see the data shown in Fig. 4 for 248 and 268 K). From Eq. (3), the slope of the lines is $2x$. The mean slope taken from all temperatures is 0.25 ± 0.03, indicating a growth exponent of $\frac{1}{8}$. Some minor deviations from power-law growth (refer, e.g., to Fig. 5) take place both at the early stage and at very late stages. In the latter case, there are indications that the domain growth becomes slower.

Figure 5 shows $I_0(t)$ vs $t^{0.25}$ for the 276-, 268-, and 261-K anneals. From the slopes of the 248- (not shown),

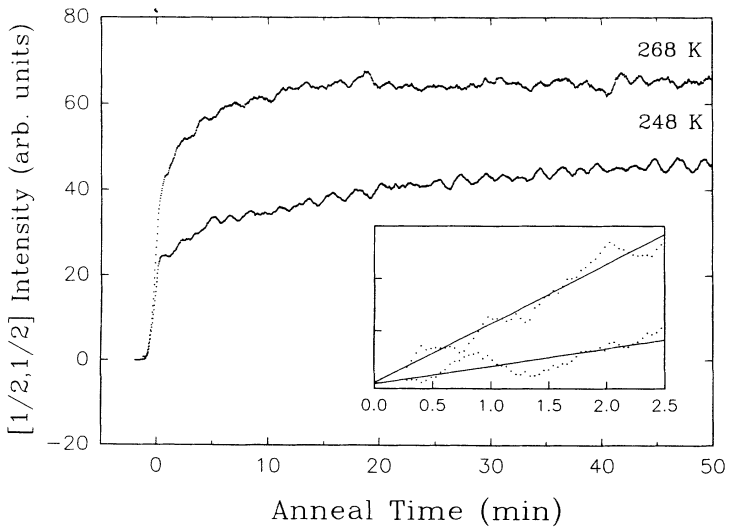

FIG. 2. Integrated LEED intensities for anneals to 248 and 268 K. The inset shows the intensities early in the anneal after subtraction of the intensity at time zero.

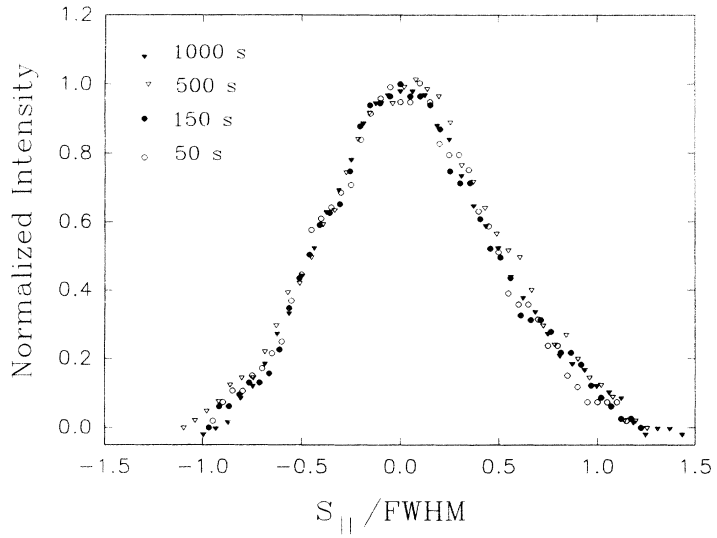

FIG. 3. LEED spot profiles taken at various times during the 276-K anneal showing scaling behavior. The peak heights are normalized and the parallel momentum transfer is scaled by dividing by the FWHM.

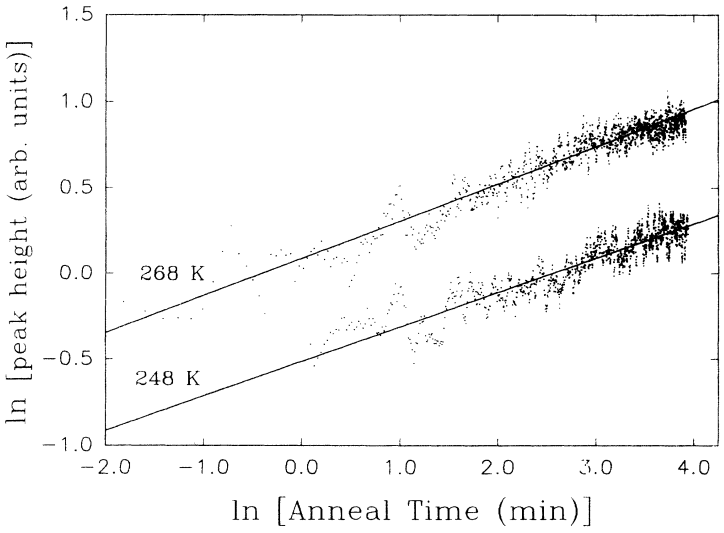

FIG. 4. Natural logarithm of the peak height as a function of the natural logarithm of the anneal time for anneals to 248 and 268 K.

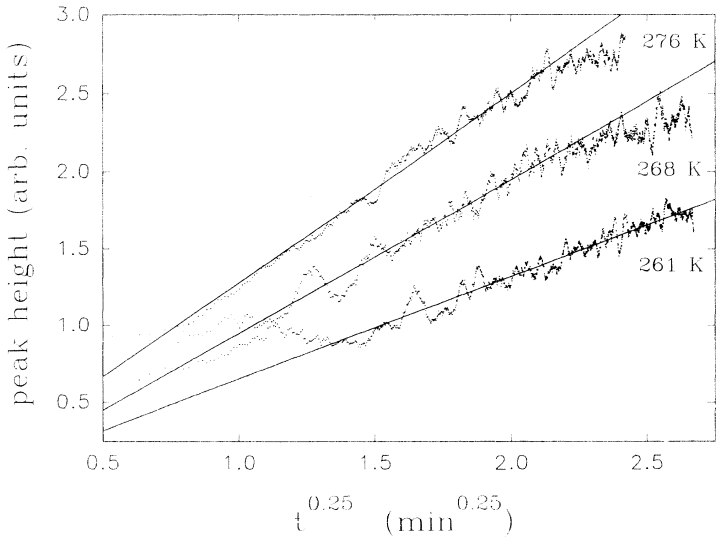

FIG. 5. LEED peak height as a function of $t^{0.25}$ for the 276-, 268-, and 261-K anneals.

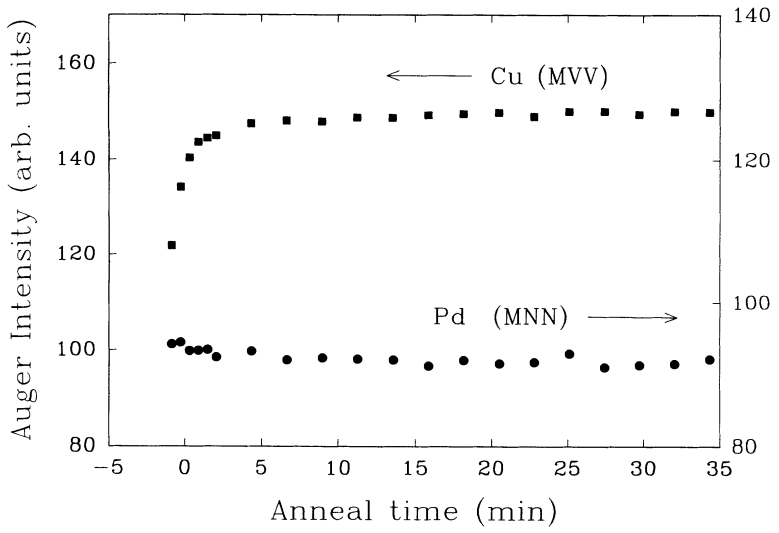

FIG. 6. Intensities of the Cu(57,60) and Pd(326,330) Auger peaks as functions of anneal time at 285 K.

261-, 268-, and 276-K curves the apparent activation energy, corresponding to the factor $A^2(T)$ in Eq. (3), is calculated to be 0.22 ± 0.01 eV.

B. AES

The intensities of the Cu(57,60) and Pd(326,330) Auger peaks are shown in Fig. 6 as functions of anneal time at 285 K. Like the integrated LEED intensity, the Cu(57,60) Auger intensity increases rapidly in the temperature ramp region. It increases more slowly for the first few minutes of the anneal before leveling off at 123% of its original intensity. The Pd(326,330) intensity appears to drop in the early stages of the anneal. There was no measurable change in the Cu(920) Auger intensity. The correlation between the increase in the Cu(57,60) intensity and the increase in the intensity of the half-order LEED beams is evidence for surface alloy formation by place exchange between Pd adsorbates and the Cu(100) surface. The Cu(57,60) intensity is most sensitive to this surface process because of the small mean free path of the 60-eV electrons.

C. Electron work-function measurements

Figure 7 shows the change in electron work function ($\Delta\Phi$) as a function of anneal time for a short anneal at 285 K. A drop in $\Delta\Phi$ is expected if the surface becomes enriched in Cu. Following an initial slight increase in the early ramp region, $\Delta\Phi$ drops sharply over the first 0.2 min of the anneal. It continues to drop slowly as the anneal proceeds. The inset of Fig. 7 exhibits the LEED intensity of Fig. 1 for short anneal times. Except for the increase in $\Delta\Phi$ in the early temperature ramp region, the work-function data mirror the LEED data. This confirms the view that the development of LEED intensity early in the anneal is due to surface alloy formation by place exchange of Pd with the Cu(100) surface. The increase of $\Delta\Phi$ in the early ramp region is difficult to explain. Neither variation in the heating current (the effects of which were carefully nulled) nor the desorption of CO or hydrogen contaminants (which would decrease $\Delta\Phi$) can account for this increase. The initial increase might be associated with desorption of minor amounts of adsorbed water, or with decreased surface roughness.

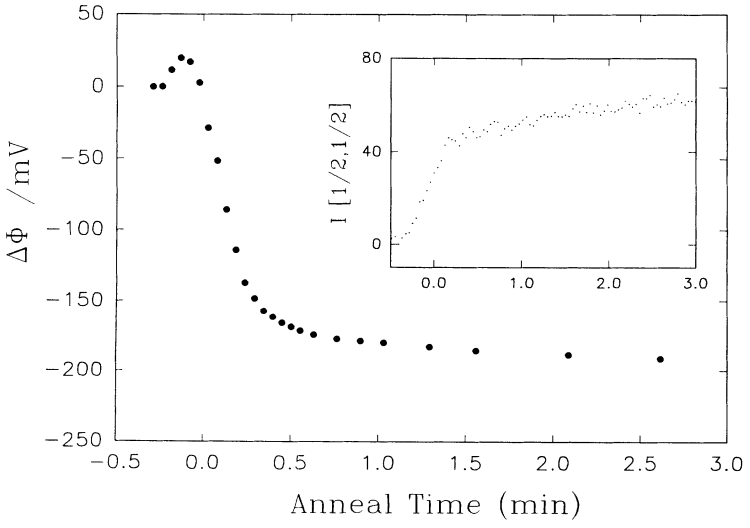

FIG. 7. Change in electron work function ($\Delta\Phi$) as a function of anneal time at 285 K. The inset shows the LEED intensity of Fig. 1 for short anneal times.

In some experiments, after a long anneal at a given temperature T_1, the temperature was ramped to a new, higher value T_2. For T_2 less than approximately 325 K this resulted in a second nonlinear increase in the LEED integrated intensity accompanied by a further drop in $\Delta\Phi$. This observation indicates that at higher temperatures additional Pd may enter the alloy layer. For T_2 above 400 K, the LEED intensity drops immediately as Pd diffusion towards the bulk becomes important. For $325 < T_2 < 400$ K, the intensity may increase initially and then decrease at longer anneal times. Preliminary data suggest that the final LEED intensity at T_2 is less than that for an anneal *directly* to T_2.

D. Thermal-desorption measurements

Hydrogen chemisorption was used as an additional probe of the state of the surface during the anneal treatments. Hydrogen does not dissociatively adsorb on Cu(100), while it does so readily on Pd(100). Desorption of hydrogen from Pd(100) is characterized by a main desorption peak at 355 K and a shoulder centered near 275 K.[18] Attard and King[19] showed that hydrogen adsorption on W(100) is blocked by the formation of $c(2\times2)$ surface alloys with the noble metals. We find that the Cu(100)-$c(2\times2)$Pd alloy formed by *room-temperature* Pd deposition also does not dissociatively adsorb hydrogen. Previous studies of hydrogen chemisorption on bimetallic systems suggest that a cluster of at least four reactive atoms is required to adsorb hydrogen.[20] They also show that spillover does not occur. We therefore expect that the amount of hydrogen adsorbed will be proportional to the number of Pd atoms in the close-packed state in islands above the Cu(100) surface.

Thermal-desorption spectra for saturation hydrogen exposure on three 0.5 ML Pd/Cu(100) alloy surfaces are shown in Fig. 8. Curve (a) corresponds to desorption from the surface as deposited at 100 K. Curve (b) exhibits desorption from a surface prepared as in (a) but ramped to 280 K and immediately cooled back down to 100 K before hydrogen exposure. The state of the surface is then similar to that at time zero in the LEED, AES, and work-function measurements. Curve (c) shows desorption from a surface prepared as in (a) but annealed at 280 K for 1 h before hydrogen exposure at 100 K.

The hydrogen desorption spectrum of curve (a) exhibits a broad desorption feature with peaks centered near 200, 250, and 290 K. The center of the desorption features is shifted about 70 K below the corresponding Pd(100) features, and the lower-temperature state dominates. A downward shift in thermal-desorption features, observed for hydrogen adsorption on Pd monolayers over other metals,[21] correlates with the positive core-level shift of a Pd atom on Cu(100).[2] A further indication of modified interaction between Pd and hydrogen on the alloy surface is the very small $\Delta\Phi$ at saturation. The saturation $\Delta\Phi$ is +200 mV on Pd(100) and only +25 mV for 0.5 ML Pd on Cu(100) at 100 K. The increase in the relative population of the lower-temperature adsorption sites may be related to the poor order in the 100-K Pd overlayer.

Following a brief ramp to 280 K, the hydrogen desorption spectrum [curve (b)] changes considerably. The integral intensity drops to about 18% of that of curve (a), and only the high-temperature desorption peak remains. We conclude that about 82% of the Pd originally present in islands on the Cu(100) surface has already formed alloy nuclei in the first substrate layer or in the periphery of Pd islands. The remaining Pd is close packed in the centers of islands. This is consistent with the LEED observation that by $t=0$, most of the half-order integrated intensity has already developed.

After 1 h at 280 K [curve (c)], the desorption peak area has dropped to 5% of that of curve (a). A minor amount of Pd must therefore remain in the close-packed state in clusters on the surface.

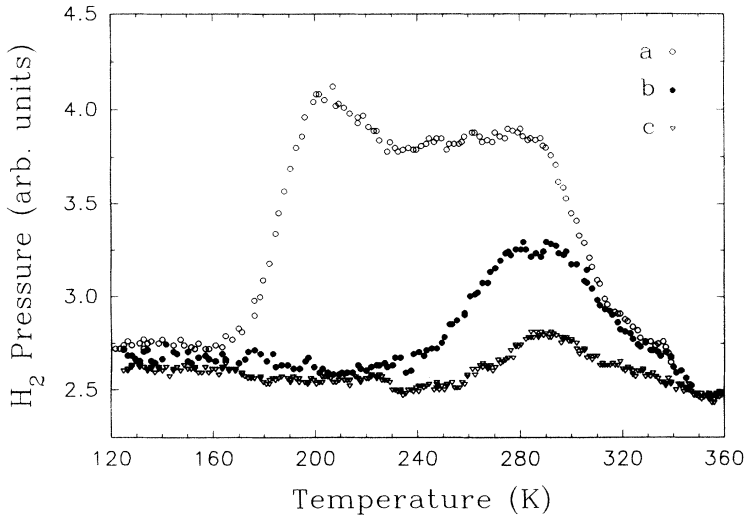

FIG. 8. Thermal-desorption spectra for saturation hydrogen exposure on three 0.5 ML Pd/Cu(100) alloy surfaces; (a) as deposited at 100 K, (b) after a very brief anneal at 280 K, and (c) after a long anneal at 280 K.

The thermal-desorption data are again consistent with the view that atomic exchange occurs rapidly early in the anneal cycle, becoming much slower at longer anneal times.

IV. DISCUSSION

A. General comments

As we have already mentioned in the Introduction, the well-established results in the theory of domain growth belong to Lifshits and Slyozov[5] and Allen and Cahn.[6] In particular, Lifshitz and Slyozov analyzed grain growth in the course of first-order phase transitions. Their mean-field kinetic theory is applicable to the late stages of coarsening of grains of one phase (the dense liquid phase) in a sea of the other (dilute gas) phase, in the limit of small density of grains. The growth mechanism involves 3D evaporation/condensation, and the growth law is given by[5,8,22]

$$R(t)\sim(\sigma v c_{\rm eq} D t/T)^{1/3}\ , \tag{4}$$

where σ is the interphase surface tension, v the atomic volume, $c_{\rm eq}$ the equilibrium gas-phase concentration, and D the diffusion coefficient. According to Eq. (4), the growth exponent is $x=\frac{1}{3}$. Substituting expression (4) into Eq. (2) shows that the apparent activation energy corresponding to the factor $A^2(T)$ in Eq. (3) can be represented as

$$E_a=2x(E_{\rm ev}+E_d)=\tfrac{2}{3}(E_{\rm ev}+E_d)\ , \tag{5}$$

where $E_{\rm ev}$ and E_d are the evaporation energy and the activation energy for diffusion, respectively. There have been subsequent efforts to extend the theory to finite density of grains, which involve intersections of grains (see the review[8]). There is agreement that $x=\frac{1}{3}$ irrespective of the density. For 2D domain growth, the Lifshits-Slyozov law should in principle be corrected,[8] but the corrections are minor (logarithmic).

Allen and Cahn[6] analyzed the kinetics of continuous phase transitions with the doubly degenerate ground state. Antiphase boundary motion has been described by employing a phenomenological Landau-Ginzburg equation without noise for a nonconserved order parameter. In this case, the growth exponent is $x=\frac{1}{2}$, i.e.,

$$R(t)\sim(Mt)^{1/2}\ , \tag{6}$$

where M is the kinetic coefficient in the Landau-Ginzburg equation. If the domain growth is connected with diffusion, the parameter M is expected to have the same activation energy as the diffusion coefficient. Accordingly, the apparent activation energy corresponding to the factor $A^2(T)$ in Eq. (3) can be represented as

$$E_a=2xE_d=E_d\ . \tag{7}$$

The order-disorder Cu(100)-$c(2\times2)$Pd phase transition with a doubly degenerate ground state formally belongs to the Allen-Cahn universal class, and one might expect $x=\frac{1}{2}$ for this case. Physically, however, this phase transition seems to have a more complex scenario compared to that described by Allen and Cahn, because the initial conditions and accordingly the growth mechanisms are different. The initial state corresponding to the Allen-Cahn theory is a two-dimensional layer containing 50% Cu and 50% Pd atoms, which are located almost randomly. In our study, we start from adsorption of 0.5 ML of Pd on the (100) face of Cu at low temperature (100 K). At first, Pd atoms are located in the adsorbed overlayer above the substrate. The initial condition for the phase transition is then formed by heating the adsorbate/substrate system up to a desired temperature (250–300 K). In this case, the initial conditions and the mechanism of the consequent domain growth, dependent on the relationship between the rates of the various elementary steps involved in the phase transition, do not correspond to those assumed in the Allen-Cahn model.

B. Elementary step and energetic

To discern the different elementary steps, we need to know their energetics. At present, accurate data on the activation energies for different rearrangements of Pd and Cu atoms on Cu(100) are lacking (experimental[23–26] and theoretical[27–32] values of the activation barriers are available only for self-diffusion of Cu atoms). The scale of the desired activation energies can be evaluated only roughly via the nearest-neighbor metal-metal interactions. Employing the empirical potentials, constructed by Flahive and Graham,[33] we have $\varepsilon_1=0.26$ and 0.22 eV for the Cu-Cu and Pd-Pd nearest-neighbor interactions, respectively (the empirical embedded-atom method yields almost the same results[34]). A Cu-Pd potential is lacking. Considering the tendency to form the $c(2\times2)$ structure, we conclude that the value of the Cu-Pd interaction should be a little higher than a half-sum of the Cu-Cu and Pd-Pd interactions. All the potentials above are of course attractive and accordingly should be negative. For us, the sign is not important, and we use positive values.

The list of elementary steps which in principle may be involved in the phase transition under consideration is as follows.

(i) Ordinary surface diffusion of single Pd or Cu atoms with the activation energy $E_d\approx2\varepsilon_1\approx0.5$ eV [the measured activation energies for self-diffusion of Cu atoms are 0.48,[23] 0.39,[24] and 0.28 (Ref. 25) eV; the embedded-atom method predicts 0.4–0.5 (Ref. 27) and 0.67 (Ref. 30) eV; the effective medium theory yields 0.44 (Ref. 28) and 0.66 (Ref. 29) eV, respectively].

(ii) Surface diffusion of Pd or Cu via the exchange mechanism (the adatom and a neighboring atom of the underlying substrate move coherently: the latter atom moves up onto the surface as the adatom replaces it[35]). The activation energy $E_{\rm ex}$ for this step is about the same as that for ordinary diffusion. The value 0.23 eV obtained from the effective medium theory[28] seems to be too low.

(iii) Two-dimensional evaporation from islands or steps to terraces. If a two-dimensional gas is in equilibrium with islands, its coverage on a square lattice is given by

$\Theta_{eq} \approx \exp(-2\varepsilon_1/T)$ [see Eq. (3.4.5) in Ref. 8]. Accordingly, the evaporation energy is $E_{ev} \approx 2\varepsilon_1 \approx 0.5$ eV. The activation energy for evaporation depends on the arrangement of particles on the island boundaries. Roughly, this energy is about $3\varepsilon_1$, i.e., a little larger than E_{ev}.

(iv) Hopping up or down descending steps at the edges of islands. The activation energy for such transitions is usually assumed to be a little higher than that for ordinary diffusion, i.e., $E_{tr} \approx 3\varepsilon_1 \approx 0.75$ eV.

(v) Creation of a vacancy on the surface with the activation energy $E_{vac} \approx (5-6)\varepsilon_1 \approx 1.2-1.4$ eV (this estimate is very rough).

(vi) Concerted rearrangement of atoms located in the underlying substrate. The activation energy for this process is expected to be about the same as for step (v).

The important observation is that formation of the $c(2\times2)$ structure starts already at 170 K. Well-established order can be observed at $T \approx 250$ K. This means that the activation energies for the main steps involved in the domain growth are fairly low. Assuming for example the values of the preexponential factors for different steps to be "normal" (10^{13} s^{-1}), one can easily estimate that ordering at 250 K is possible only if all the activation energies are lower than 0.7 eV. Taking into account this restriction, below we ignore steps (iv)–(vi). Step (iv) in principle is not negligible, but its role is expected to be minor.

C. Initial stage of domain growth

Adsorption of 0.5 ML of Pd on Cu(100) at 100 K results in the formation of a poorly ordered Pd overlayer. With increasing temperature from 100 K up to a desired value, the arrangement of Pd and Cu atoms is controlled mainly by diffusion (two-dimensional evaporation is almost negligible in this case). As we have mentioned above, diffusion may occur via ordinary and exchange jumps. The former channel results mainly in the formation and growth of Pd islands in the adsorbed overlayer. The latter channel, supplying Cu atoms to the adsorbed overlayer and Pd atoms to the underlying substrate layer, contributes both to the formation and growth of islands and to the creation of nuclei of the $c(2\times2)$ phase.

The activation energies for ordinary and exchange diffusion are expected to be close[35] and *a priori* it is difficult to favor one channel or another. There are, however, experimental possibilities to reveal the relative roles of these channels by measuring the kinetics of alloy formation in temperature-programmed regimes with different heating rates. Physically, it is clear that at low temperatures the dominant channel is that with lower activation energy, and with increasing temperature, the relative difference between their rates will be reduced. Ordinary diffusion resulting in formation of Pd islands inhibits creation of alloy nuclei. If the activation energy for ordinary diffusion is lower than for exchange jumps, the dominant role of this diffusion at low temperatures can be suppressed somewhat by increasing the heating rate. In this case, one can expect that the higher the heating rate, the better the $c(2\times2)$ order. This is just the case observed in our preliminary studies, where pausing at lower temperature resulted in poorer $c(2\times2)$ order. Thus, ordinary diffusion seems to be slightly more favorable than exchange jumps. This conclusion is supported by *ab initio* LDA calculations,[32] and by extrapolating results obtained by molecular-dynamics simulations with embedded-atom potentials from 900 and 600 K to 300 K.[31(c)] Under such circumstances, the initial condition for the phase transition is assumed to be a set of small islands containing primarily Pd atoms.

At the temperatures where the kinetics of domain growth have been studied, the rates of ordinary and exchange diffusion are expected to be comparable. The early stages of domain growth are connected with exchange diffusion and destruction of smaller Pd islands. Both of these processes, already starting during heating, are relatively rapid (compared to evaporation from large islands) and accordingly the early stage of the phase transition is rather fast. During this stage, a considerable fraction of the Pd migrates via exchange jumps to the first substrate layer. In some sense, the beginning of surface alloy formation described above resembles the early stage of the Allen-Cahn scenario because the process is not limited by evaporation.

Any universal results for such early stages of the order-disorder phase transitions are known to be lacking. In principle, one can employ here Monte Carlo simulations. At realistic values of the different parameters, these approaches are, however, too time consuming. We will restrict our analysis of the early stage of domain growth only by formal application of Eqs. (6) and (7). Such an application is not quite justified. Nevertheless, the result obtained, $E_{ex} \approx 0.34$ eV, compares favorably with recent experimental and theoretical results (Sec. IV B).

D. Late stage of domain growth

At the late stage of domain growth, the mean sizes of Pd islands and $c(2\times2)$ domains, $r(t)$ and $R(t)$, become relatively large. Accordingly, the growth kinetics become slow. To describe the late stage of the kinetics, we should take into account that the domain and island growths are interconnected. In particular, Pd atoms evaporated from islands will primarily be captured via exchange diffusion by $c(2\times2)$ domains located in the first substrate layer because this layer is undersaturated by Pd. Cu atoms supplied to the adsorbed overlayer via exchange will be primarily trapped by large islands. Thus, the periphery and even centers of large Pd islands will contain a considerable amount of Cu atoms, as indicated by AES, Fig. 5. Accordingly, the $c(2\times2)$ domains will start to grow in these regions as well.

We will assume the domain growth to occur mainly in the first substrate layer. By analogy with the Allen-Cahn theory, the rate of domain growth is expected to be proportional to the product of the diffusion coefficient and the mean curvature of the domain boundaries. In addition, since the first substrate layer is undersaturated by Pd, we assume the domain growth to be limited by evaporation of Pd atoms from islands which are oversaturated by Pd. In other words, the growth rate is proportional

to the average coverage of the surface by Pd atoms in the regions that are not covered by islands, Θ_g (physically this coverage corresponds to the two-dimensional Pd-gas phase). Thus, we have the following equation for the domain growth:

$$dR/dt \sim D\Theta_g/R \ , \tag{8}$$

where D is the coefficient for exchange diffusion. Note that below, the designation D is employed also for other diffusion coefficients, because the orders of magnitude of different diffusion coefficients are considered to be the same.

The coverage Θ_g can be calculated from the balance between evaporation of Pd atoms from islands and adsorption of these atoms by the first substrate layer. To obtain the balance equation, we should first describe the evolution of islands.

As pointed out above, the periphery of islands should contain a considerable amount of Cu atoms. For this reason, we will assume the two-dimensional Cu gas to be almost in equilibrium with Cu atoms located in other phases. In this case, the growth of islands is controlled mainly by evaporation and condensation of Cu atoms on their periphery. To describe this process, we employ an equation of the Lifshits-Slyozov type,

$$r \sim (\Theta_{eq} Dt)^{1/3} \ , \tag{9}$$

where Θ_{eq} is the equilibrium coverage corresponding to the two-dimensional Cu-gas phase. In fact, Eq. (9) is the same as (4) (we only omit all the factors which have no Arrhenius dependence on temperature). Using Eq. (9), it is possible to calculate the other average characteristics of islands. For example, the total number of islands is inversely proportional to the area of an island,

$$N \sim 1/r^2 \ . \tag{10}$$

For the total perimeter of islands, we have

$$L \sim rN \sim 1/r \ . \tag{11}$$

According to the Lifshits-Slyozov scenario, larger islands grow at the expense of smaller ones. In other words, the size of small islands decreases with increasing time. Thus, evaporation of Pd atoms is expected to occur primarily from these islands. Assuming the perimeter of small islands to be proportional to the total perimeter of islands, we have the following equation for the total flux of Pd atoms evaporated from small islands:

$$F \sim LD\Theta_{eq}/r \ , \tag{12}$$

where Θ_{eq} is the equilibrium coverage corresponding to the two-dimensional Pd-gas phase (we use the same symbol Θ_{eq} both for Pd and Cu because the orders of magnitude of these two coverages are the same). Physically, the right-hand part of Eq. (12) is just a product of the total perimeter and the diffusion flux per unit length of the island boundary. Calculating the diffusion flux, we assume the equilibrium Pd-gas coverage near the boundary (as in the Lifshits-Slyozov theory). Then, the scale of the coverage gradient is Θ_{eq}/r, and accordingly the scale of the diffusion flux per unit length is $D\Theta_{eq}/r$.

The rate of absorption of Pd atoms by the first substrate layer is proportional to the product of the diffusion coefficient and the average coverage of the surface by Pd atoms in the regions that are not covered by islands, i.e.,

$$W \sim D\Theta_g \ . \tag{13}$$

The domain growth is slow, and at the late stage there is a balance between evaporation and absorption, i.e.,

$$F \approx W \ . \tag{14}$$

Substituting into this equation expressions (12) and (13) yields for the coverage Θ_g

$$\Theta_g \sim L\Theta_{eq}/r \ . \tag{15}$$

Employing then expressions (9) and (11) for r and L, we can rewrite Eq. (15) as

$$\Theta_g \sim \Theta_{eq}^{1/3}(Dt)^{-2/3} \ . \tag{16}$$

Substituting expression (16) into Eq. (8) yields

$$dR/dt \sim (D\Theta_{eq})^{1/3} t^{-2/3}/R \ . \tag{17}$$

Integrating this equation, we obtain the following growth law for our model:

$$R(t) \sim (\Theta_{eq} Dt)^{1/6} \ . \tag{18}$$

Thus, the growth exponent predicted is $x=\frac{1}{6}$. Substituting expression (18) into Eq. (2) shows that the apparent activation energy corresponding to the factor $A^2(T)$ in Eq. (3) can be represented in our case as

$$E_a = 2x(E_{ev}+E_d) = \tfrac{1}{3}(E_{ev}+E_d) \ . \tag{19}$$

From Eqs. (18) and (19), we make the following two important conclusions. (i) The observed low value of the growth exponent ($x=\frac{1}{8}$) can really occur if the Pd-Cu ordering of the Allen-Cahn type is limited by the dissolution of Pd islands occurring via the Lifshitz-Slyozov scenario. In particular, our scaling analysis predicts $x=\frac{1}{6}$. The latter value is close to $\frac{1}{8}$. (ii) Dividing the apparent activation energy E_a by $2x$, we should obtain $(E_{ev}+E_d)$. Employing the experimental values $E_a=0.22$ eV and $2x=\frac{1}{4}$, we have $E_{ev}+E_d=0.88$ eV. If $E_{ev}\approx E_d$ (see Sec. IV B), the activation energy for surface diffusion, estimated from the domain-growth kinetics, is $E_d \approx 0.44$ eV. This value is reasonable (see Sec. IV B). The latter indicates that our model is self-consistent.

Comparing the experimental and theoretical results, it is of interest to discuss in more detail some limitations of our scaling analysis above and to clarify the possible reasons why the exponent obtained ($x=\frac{1}{6}$) is slightly larger than the measured one ($x=\frac{1}{8}$). There are at least two phenomena that might be involved in the phase transition and were ignored in our model. The first one is the formation of $c(2\times2)$ domains inside Pd islands due to hopping of Cu atoms from the adsorbed overlayer up descending steps at the edges of islands and then Cu-Pd exchange (this channel has already been mentioned in Sec. IV B). The second phenomenon is connected with the is-

land growth. Our model takes into account this process but ignores the fact that the rearrangement of island boundaries due to evaporation and condensation eventually results in the situation where a fraction of Pd atoms is located *below* islands. Such "covered" Pd atoms have been observed in medium energy ion scattering (MEIS) studies of Cu(100)-$c(2\times2)$Pd.[36] These Pd atoms are at least temporarily unable to participate in the ordering process. Effectively, the Pd/Cu ratio becomes lower than the optimum one (50/50). With increasing time, this effect is more and more important. The latter may result in a decrease in the growth exponent and even in minor deviations from power-law growth as observed in the experiment (Sec. III A).

E. Comparison with surface ordering of a bulk $Cu_3Au(100)$ crystal

As pointed out in the Introduction, studies of the kinetics of domain growth during the formation of surface alloys so far have been lacking. There are, however, the experimental data of McRae and Malic[16] (MM) on the kinetics of surface ordering of a bulk Cu_3Au crystal. They observed two distinct ordering regions. The first one, characterized by a linear increase in the LEED peak height, was assumed to be connected with nucleation of microclusters. The second one, in which power-law growth was observed, was attributed to domain growth by the elimination of domain boundaries. The observed kinetics of ordering of the surface of the bulk alloy is therefore qualitatively the same as that measured in our study. For the bulk alloy case, however, the apparent activation energies reported by MM for nucleation and domain growth, 1.8 and 1.6 eV, are much higher than in our case. This is because nucleation and domain growth for the $Cu_3Au(110)$ surface both require intralayer rearrangement, while in our case these processes may proceed via a more facile surface atom exchange. The (2×1) structure which develops on the $Cu_3Au(110)$ surface is twofold degenerate, and again one might expect a growth exponent of $\frac{1}{2}$ for power-law growth. MM report an exponent of $\frac{1}{4}$, significantly below the anticipated value. They tentatively associated this with the presence of extra domain walls due to surface segregation of Au, but did not present a kinetic scheme illustrating this effect.

V. SUMMARY

Employing LEED, AES, and other techniques, we have studied the kinetics of formation of the Cu(100)-$c(2\times2)$Pd surface alloy at 248–276 K. The initial stage of this process is found to be rapid and short. The subsequent late stage, where the domain growth is self-similar, is slow. In the latter case, the growth law for the average domain radius has a power-law form with an exponent of $\frac{1}{8}$. Scaling analysis shows that such a low value of the growth exponent can really take place if the Pd-Cu ordering is limited by dissolution of Pd islands. In the latter case, the apparent activation energy for the LEED intensity is equal to the sum of the activation energies for surface diffusion and for two-dimensional evaporation from islands. The activation barrier for surface diffusion in the domain-growth regime is estimated to be ≈ 0.4 eV.

ACKNOWLEDGMENTS

This work was funded by the Natural Sciences and Engineering Research Council of Canada and the Network of Centres of Excellence in Molecular and Interfacial Dynamics (CEMAID). One of us (V.P.Zh.) thanks the Centre for Interdisciplinary Studies in Chemical Physics at the University of Western Ontario for financial support. We also wish to acknowledge P. Piercy for helpful discussions, and J. E. Black and Z. J. Tian for presenting the results of their calculations before publication.

*On leave from Institute of Catalysis, Novosibirsk 630090, Russia.

[1]T. Flores, M. Hansen, and M. Wuttig, Surf. Sci. **279**, 251 (1992); L. Pleth Nielsen, F. Besenbacher, I. Stensgaard, E. Laegsgaard, C. Engdahl, P. Stoltze, K. W. Jacobsen, and J. K. Norskov, Phys. Rev. Lett. **71**, 754 (1993); Q. Jiang, Y.-L. He, and G.-C. Wang, Surf. Sci. **295**, 197 (1993).

[2]T. D. Pope, K. Griffiths, and P. R. Norton, Surf. Sci. **306**, 294 (1994).

[3]T. J. Raeker and A. E. DePristo, J. Vac. Sci. Technol. A **10**, 2396 (1992).

[4]J. Kudrnovsky, S. K. Bose, and V. Drchal, Phys. Rev. Lett. **69**, 308 (1992); J. E. Black, Phys. Rev. B **46**, 4292 (1992).

[5]I. M. Lifshitz and V. V. Slyozov, J. Phys. Chem. Solids **19**, 35 (1961).

[6]S. M. Allen and J. W. Cahn, Acta Metall. **27**, 1085 (1979).

[7]A. Sadiq and K. Binder, J. Stat. Phys. **35**, 517 (1984).

[8]V. P. Zhdanov, *Elementary Physicochemical Processes on Solid Surface* (Plenum, New York, 1991), pp. 214–230.

[9]V. P. Zhdanov, Surf. Sci. **194**, L100 (1988).

[10]P. K. Wu, M. C. Tringides, and M. G. Lagally, Phys. Rev. B **39**, 7595 (1989).

[11]M. C. Tringides and M. G. Lagally, in *Reflection High Energy Diffraction and Electron Imaging of Surfaces,* edited by P. K. Larsen and P. Dobson (Plenum, New York, 1988).

[12]M. C. Tringides, Phys. Rev. Lett. **65**, 1372 (1990).

[13]J.-K. Zuo, G.-C. Wang, and T.-M. Lu, Phys. Rev. B **39**, 9432 (1989); G.-C. Wng, J.-K. Zuo, and T.-M. Lu, in *Phase Transitions in Surface Films 2,* edited by H. Taub *et al.* (Plenum, New York, 1991), pp. 455–470.

[14]M. Witt and E. Bauer, Ber. Bunsenges Phys. Chem. **90**, 248 (1986).

[15]G. W. Graham, Surf. Sci. **171**, L432 (1986); S. C. Wu, S. H. Lu, Z. Q. Wang, C. K. C. Lok, J. Quinn, Y. S. Li, D. Tian, F. Jona, and P. M. Marcus, Phys. Rev. B **38**, 5363 (1988).

[16]E. G. McRae and R. A. Malic, Phys. Rev. B **42**, 1509 (1990).

[17]T. D. Pope, G. W. Anderson, K. Griffiths, P. R. Norton, and G. W. Graham, Phys. Rev. B **44**, 11 518 (1991).

[18]R. J. Behm, K. Christmann, and G. Ertl, Surf. Sci. **99**, 320 (1980).

[19]G. A. Attard and D. A. King, Surf. Sci. **223**, 1 (1989).
[20]K. Christmann, Surf. Sci. Rep. **9**, 1 (1988).
[21]J. M. Heitzinger, S. C. Gebhard, and B. E. Koel, Chem. Phys. Lett. **200**, 65 (1992).
[22]E. M. Lifshitz and L. P. Pitaevskki, *Physical Kinetics* (Pergamon, Oxford, 1981), Chap. XII.
[23]J. J. de Miguel, A. Cebollada, J. M. Gallego, J. Ferron, and S. Ferrer, J. Cryst. Growth **88**, 442 (1988).
[24]M. Breeman and D. O. Boerma, Surf. Sci. **269**, 224 (1992).
[25]H.-J. Ernst, F. Fabre, and J. Lapujoulade, Phys. Rev. B **46**, 1929 (1992).
[26]M. T. Kief and W. F. Egelhoff, Jr., Phys. Rev. B **47**, 10785 (1993).
[27]C. L. Liu, J. M. Cohen, J. B. Adams, and A. F. Voter, Surf. Sci. **253**, 334 (1991).
[28]L. B. Hansen, P. Stoltze, K. W. Jacobsen, and J. K. Norskov, Phys. Rev. B **44**, 6523 (1991); Surf. Sci. **289**, 68 (1993).
[29]D. E. Sanders and A. E. DePristo, Surf. Sci. **260**, 116 (1992).
[30]M. Breeman and D. O. Boerma, Surf. Sci. **287**, 881 (1993).
[31]J. E. Black and Z. J. Tian, (a) Phys. Rev. Lett. **71**, 2445 (1993); (b) Comments Condens. Matter Phys. **16**, 281 (1993); (c) private communication.
[32]C. Lee, G. T. Barkema, M. Breeman, A. Pasquarello, and R. Car, Surf. Sci. **306**, L575 (1994).
[33]P. G. Flahive and W. R. Graham, Surf. Sci. **91**, 449 (1980).
[34]V. P. Zhdanov (unpublished results).
[35]P. J. Feibelman, Comments Condens. Matter Phys. **16**, 191 (1993).
[36]T. D. Pope, M. Vos, H.-T. Tang, K. Griffiths, I. V. Mitchell, P. R. Norton, W. Liu, Y. S. Li, K. A. R. Mitchell, Z.-J. Tian, and J. E. Black (unpublished).